Available online at www.sciencedirect.com
SCIENCE DIRECT®
Journal of Magnetic Resonance 166 (2004) 100–110
JMR Journal of Magnetic Resonance
www.elsevier.com/locate/jmr

Multiple-spin analysis of chemical-shift-selective (^{13}C, ^{13}C) transfer in uniformly labeled biomolecules

Lars Sonnenberg,[1] Sorin Luca,[2] and Marc Baldus*

Department for NMR-Based Structural Biology, Max-Planck-Institute for Biophysical Chemistry, 37077 Göttingen, Germany

Received 17 July 2003; revised 20 October 2003

Abstract

Chemical-shift-selective (^{13}C, ^{13}C) polarization transfer is analyzed in uniformly labeled biomolecules. It is shown that the spin system dynamics remain sensitive to the distance of interest and can be well reproduced within a quantum-mechanical multiple-spin analysis. These results lead to a general approach on how to describe chemical-shift-selective transfer in uniformly labeled systems. As demonstrated in the case of ubiquitin, this methodology can be used to detect long-range distance constraints in uniformly labeled proteins.

Keywords: Distances; MAS; Polypeptides; Solid-state; Structure determination

1. Introduction

The detection of through-space contacts represents one of the primary instruments of nuclear magnetic resonance (NMR) to probe structural parameters in soluble or solid-phase molecules. In the latter case, the dipolar coupling appears explicitly in the system Hamiltonian and directly encodes the interatomic distance between two nuclei [1]. In the presence of additional anisotropic interactions such as the chemical shielding and dipolar couplings, an exact determination of the intermolecular distance is in general difficult and the application of standard high-resolution methods such (i.e. magic angle spinning MAS [2]) to remove anisotropic contributions is mandatory. Dipolar recoupling methods can subsequently be employed [3–5] to detect through-space interactions with high spectral resolution. Numerous biophysical applications attest to the efficiency of these methods to address a particular structural problem in an insoluble and non-crystalline environment (see [6–8] for recent reviews).

Perhaps the easiest and most widely used solid-state NMR method to determine a homonuclear dipolar coupling refers to the rotational resonance (RR) phenomenon [9–12] where MAS rate and the isotropic chemical shift difference fulfill well-defined selection rules. This dipolar recoupling technique represents the prototype of a chemical-shift-selective (CSS) polarization transfer method to determine an internuclear distance of interest. Even in the case of a selectively labeled spin pair, experimental and theoretical results indicate that the structural interpretation of the resulting NMR data must usually include multiple-spin effects due to surrounding (highly abundant) proton spins [13,14]. For RR [13–20] and other CSS transfer methods [21–23], these additional multiple-spin interactions have been treated as a source of relaxation during the transfer process.

If one is interested in measuring multiple structural parameters or to determine the complete 3D structure of a molecule of interest, the study of doubly labeled specimens can become tedious and NMR methods that yield distance constraints in a single uniformly labeled molecule are particularly appealing. Here, considerable progress has recently been made regarding the spectral

* Corresponding author. Fax: +49-551-201-2202.
E-mail address: maba@mpibpc.mpg.de (M. Baldus).
[1] Present address: Lehrstuhl für Angewandte Physik, Ludwig-Maximilians Universität, 80799 München, Germany.
[2] Present address: Laboratory of Molecular Biology, NIDDK, NIH, Bethesda, MD 20892-8030, USA.

1090-7807/$ - see front matter © 2003 Elsevier Inc. All rights reserved.
doi:10.1016/j.jmr.2003.10.014

assignment of proteins [24–28] and membrane proteins [29–32], for example providing the basis for the 3D structure determination of a ^{13}C block-labeled 63-residue protein [33]. Although CSS transfer methods have already been successfully utilized in the context of small peptides [34–36] and studied in three-spin cases [37], a further understanding of which spin system parameters affect CSS transfer dynamics, in particular in the case of larger systems, is desirable.

Meier and co-workers [19] have recently proposed to describe rotational resonance transfer in a uniformly labeled amino acid by an effective two-spin system (characterized by the dipolar coupling of interest and the zero-quantum relaxation rate T_2^{ZQ}) and a phenomenological offset in the final difference polarization that reflects the strongly coupled environment. As recently shown by Costa et al. [20], insufficient ^1H decoupling may lead to a regime where zero-quantum relaxation dominates the transfer dynamics. In this case, the final difference polarization vanishes and an accurate detection of the dipolar coupling of interest is difficult. Moreover, an extension of a relaxation-based concept to the case of a radio-frequency driven transfer method may require the inclusion of additional free parameters (such as T_1^{ρ}) to describe the transfer dynamics during mixing.

For these reasons, we explore in the following an alternative route to monitor the spin system dynamics under CSS transfer by conducting a full Hilbert-space analysis of a strongly coupled (^1H, ^{13}C) spin system. While analytical functions [5,38] have previously been obtained for dipolar coupled three- and four-spin systems in the context of cross-polarization [39,40] transfer, we here resort to numerical simulations within the QM simulation routine GAMMA [41] to study CSS transfer among up to nine dipolar and scalar coupled spins. To test the validity of our multiple-spin (in the following referred to as MS) approach, we first compare the experimental results of CSS transfer under RR conditions in small model systems of known structure to the numerical predictions. Subsequently, we investigate whether the resulting transfer curves remain sensitive to the structural parameter of interest. These results suggest a general approach on how to analyze CSS transfer experiments in uniformly labeled systems of unknown structure. In contrast to a relaxation-based analysis, the MS method only relies on chemical shift assignments and standard knowledge about the spin system of interest and contains the dipolar coupling of interest as the only unknown parameter. Because the MS analysis explicitly contains interactions to a surrounding ^1H bath, we can readily monitor the influence of insufficient proton decoupling upon the transfer characteristics for variable (^{13}C, ^{13}C) distance. Moreover, the MS concept can easily be extended to the analysis of RR variants employing small radio frequency fields (RRTR [17,42,43]) during mixing. As we will demonstrate on uniformly [^{13}C, ^{15}N]-labeled ubiquitin, such methods are of advantage in the case of severe spectral overlap. Again, the MS approach permits a direct investigation of the transfer characteristics for a given set of experimental parameters and underlines the usefulness of CSS transfer for providing medium- or long-range distance constraints in larger, multiply or uniformly labeled polypeptides.

2. Materials and methods

2.1. Sample preparation

Uniformly [^{13}C, ^{15}N]-labeled L-histidine·HCl (L-His·HCl) was purchased from Cambridge Isotope Laboratories (CIL, Andover, MA) and recrystallized from aqueous solutions at 10% dilution using standard procedures. Uniformly [^{13}C, ^{15}N]-labeled ubiquitin was purchased from VLI research (Malvern) and 5 mg of the sample was placed into a 4 mm rotor and hydrated using 2 μl of H_2O.

2.2. NMR spectroscopy

Solid-state NMR experiments were conducted on 9.4 T (^1H resonance frequency: 400 MHz) and 14.1 T (600 MHz) wide-bore instruments (Bruker Biospin/Germany) using standard 4 mm triple-resonance (^1H, ^{13}C, ^{15}N) MAS probe heads. The sample temperatures were actively controlled at −5 °C (L-His·HCl) or −10 °C (ubiquitin) during the course of the experiments. Unless stated otherwise, radio frequency fields for ^1H CW or TPPM [44] decoupling were set to 83 kHz. The two NMR pulse schemes utilized in this work are shown in Fig. 1. In (A) longitudinal mixing among (^{13}C, ^{13}C) spins under rotational-resonance recoupling conditions is detected in a constant-time (CT-RR) fashion [45]. After a ramped cross-polarization [46] and a 90° pulse, a weak 180° pulse (typically 300 μs long) inverts spins close to resonance. Subsequently, zero-quantum mixing leads to a decay of difference magnetization that is monitored as function of the mixing time t_{mix} and read out after a final 90° pulse. In (B), the RRTR has been combined with short ramp-in and ramp-out pulses [17] to establish the appropriate initial condition (vide infra) for dipolar mixing. Furthermore, the method has been extended to two spectral dimensions [47] and contains a constant-time segment to minimize hardware instabilities for variable evolution and mixing times (CT-RRTR).

2.3. Theory and quantum-mechanical simulations

All quantum-mechanical (QM) simulations were performed within the C++-based NMR simulation

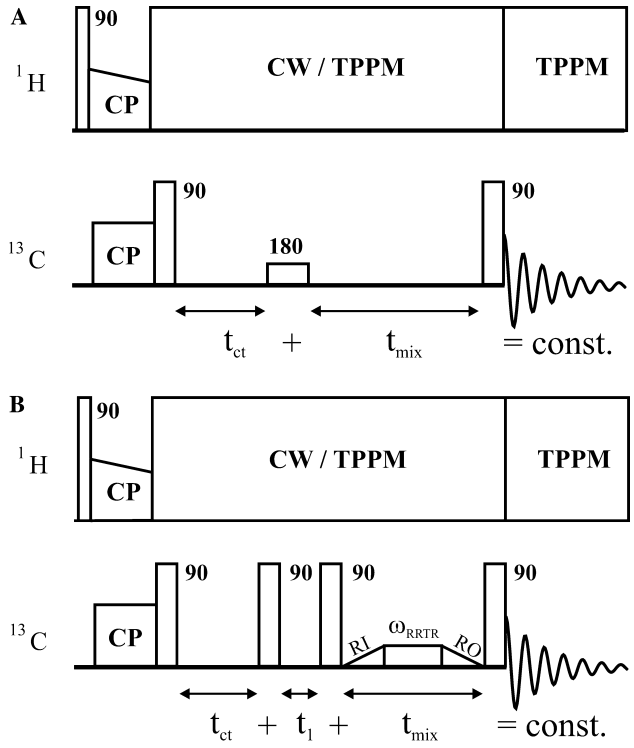

Fig. 1. (A) Constant-time 1D experiment to monitor the decay of difference magnetization under rotational resonance conditions (CT-RR) [45]. All experimental results were obtained using standard [55] phase cycling involving spin-temperature alternation and CYCLOPS (applied to the 90° pulse prior to detection). (B) Constant-time two-dimensional correlation experiment using RRTR [42,43] mixing (2D CT-RRTR). Here, CW ^{1}H decoupling was used instead of TPPM [44] whenever RF pulses were applied on the ^{13}C channel. Phase sensitive detection along t_1 was achieved using standard TPPI [55] phase cycling of the 90° pulse prior to the t_1 evolution. This preparatory (and all following) pulses furthermore were phase-cycled in steps of 90° in concert with the receiver phase. Spin-temperature alternation on the 90° ^{1}H pulse leads to a minimal, eight-step phase cycle.

environment GAMMA [41]. Internal system contributions encompass the chemical shielding (CS), the dipolar (D), and scalar (J) coupling. Using the generalized Hilbert-space Hamiltonian

$$H_{\text{int}} = \sum_{I,S} H_{\text{CS}} + H_D + H_J, \tag{1}$$

where I and S refer to ^{13}C and ^{1}H spins, respectively, one-dimensional (CS) and two-dimensional (D,J) arrays were defined to generate (rank 2) spherical space tensors in the principal axis system (PAS). The explicit definition of the spatial and spin tensor components of the relevant interactions can be found in [1,5]. Anisotropic chemical shielding interactions for all ^{13}C nuclei were taken from the literature [48] and neglected for ^{1}H spins. ^{13}C CSA interactions were also cross-validated by a Floquet analysis [49–51] of the experimentally detected MAS sideband pattern. In line with earlier studies [52], test simulations confirmed that the relative orientation of the anisotropic interactions is not relevant for the considered RR recoupling conditions. Distances defining the overall structure were taken from neutron diffraction studies (L-His · HCl [53]) and X-ray crystallography (ubiquitin [54]).

Scalar (^{1}H, ^{13}C) and (^{13}C, ^{13}C) couplings were set to 140 and 35 Hz, respectively. ^{1}H decoupling during mixing was numerically simulated under CW or TPPM condition using the following radio frequency Hamiltonian (RF):

$$H_{\text{dec}} = \begin{cases} \sum_k \omega_{S,\text{CW}} S_{kx} \\ \sum_k \omega_{S,\text{TPPM}} (S_{kx}\cos\varphi(t) + S_{ky}\sin\varphi(t)); \\ \quad \varphi(t) = \begin{cases} 0° & \text{if } \text{int}(t/\tau) = \text{even}, \\ 15° & \text{if } \text{int}(t/\tau) = \text{odd}, \end{cases} \end{cases} \tag{2}$$

where τ relates to an experimentally optimized TPPM pulse length. For RR recoupling, the MAS rate ω_{R} was set to the chemical shift difference $\Delta\Omega_{kl} = \Omega_k - \Omega_l = n\omega_{\text{R}}$ (where $n = 1$ or 2) of the (^{13}C$_k$, ^{13}C$_l$) spin pair of interest. For CT-RRTR, the RF field ω_{RRTR} fulfilled the generalized resonance conditions:

$$\omega_{\text{R}} = \sqrt{\Omega_k^2 + \omega_{\text{RRTR}}^2} + \sqrt{\Omega_l^2 + \omega_{\text{RRTR}}^2}. \tag{3}$$

All CT-RRTR correlation experiments discussed here were performed by centering the carrier frequency between the resonance frequencies of the spin pair of interest. The RF field hence directly depends on the isotropic chemical shift difference and the MAS rate via $\omega_{\text{RRTR}} = \sqrt{\omega_{\text{R}}^2 - \Delta\Omega_{kl}^2}/2$. The size of the RF recoupling field and the linear ramp-in and ramp-out pulses were incorporated into the numerical simulations, i.e.,

$$H_{\text{RRTR}}(t) = \begin{cases} \sum_k \omega_{\text{RI}}(t) I_{kx}, & 0 < t < t_{\text{RI}}, \\ \sum_k \omega_{\text{RRTR}} I_{kx}, & 0 < t - t_{\text{RI}} < t_{\text{mix}}, \\ \sum_k \omega_{\text{RO}}(t) I_{kx}, & 0 < t - t_{\text{RI}} - t_{\text{mix}} < t_{\text{RO}}. \end{cases} \tag{4}$$

The spin system dynamics were solved by numerical integration of the Liouville–von-Neumann equation [55] for time periods of 0.25 μs. The initial density operator $\sigma(0)$ and final detection operators ρ for the numerical simulation of 1D-RR and 2D-RRTR experiments were:

$$\sigma(0) = I_{1z} - I_{2z}; \quad \rho = \Delta_{12} = I_{1z} - I_{2z} \tag{5}$$

and

$$\sigma(0) = I_{1z}; \quad \rho = \Gamma_{12} = I_{2z}, \tag{6}$$

respectively. The anisotropic nature of the samples under MAS was simulated by a numerical powder integration [56] using 500 orientations. All numerical simulations were performed on a LINUX cluster using 2×3 parallel Pentium III 735 MHz processors and resulted in total simulation times of several hours (five to six spins) to one week (nine spins).

3. Results and discussion

3.1. Multiple-spin analysis

The CSS transfer analysis presented in the following is particularly useful for the investigation of interresidue contacts in polypeptides. The corresponding spin system topologies are most easily approximated by first considering uniformly labeled amino acids. In Fig. 2, we hence compare the experimentally detected CT-RR transfer curves for the Cα–Cγ spin pair in L-His · HCl to quantum-mechanical model calculations assuming three different spin geometries. The relevant spin system topologies are indicated for each simulation. In (A), an isolated two-spin system containing Cα and Cγ spins only was assumed. Clearly, the experimental data points poorly correlate with theoretical expectations. In (B), the spin system was extended to include all ^{13}C spins in L-His · HCl. Here, the experimentally observed oscillation is strongly damped in comparison to the numerical two-spin simulation making the introduction of a phenomenological zero-quantum relaxation time plausible. Nevertheless, the QM result still does not adequately reflect the empirical results. Finally (C), the spin system dynamics were computed by taking five ^{13}C spins (i.e., removing Cε1 from the calculation) and two ^{1}H spins into account. Under these conditions, the theoretical curve is in good agreement with the experimental results indicating the validity of the chosen MS approach. The remarkable difference between Figs. 2B and C underlines that CSS polarization transfer under the considered experimental conditions remains sensitive to heteronuclear (^{1}H, ^{13}C) interactions even under CW decoupling.

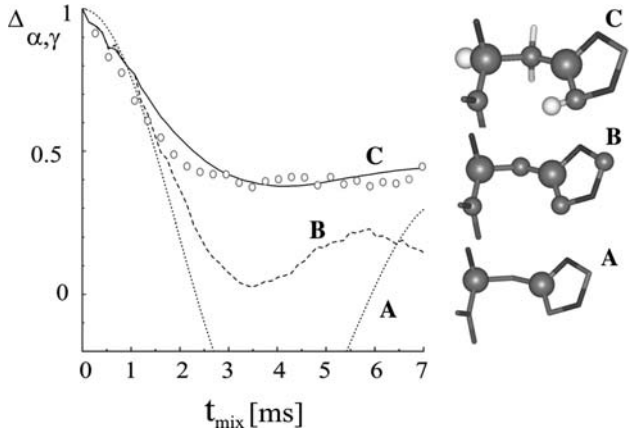

Fig. 2. Comparison between experimental CT-RR transfer curves (symbols) obtained for the Cα–Cγ pair in L-His · HCl with QM simulations including only the Cα and Cγ spin (dotted, A), six ^{13}C spins (dashed, B), and five ^{13}C and two attached protons (solid line, C). ^{13}C and ^{1}H spins included in the calculations are indicated as spheres. The carbon atoms of interest (i.e., Cα and Cγ) are enlarged. For reasons of molecular symmetry, Cβ protons are not affecting the results of the calculation in (C).

In Fig. 2, six ^{13}C spins were considered in (B) while the curve (C) involves five ^{13}C spins and two additional ^{1}H spins leading to a total spin system size of seven spins. We note that a further increase in the spin system size does not alter the results of the calculation.

In a more general sense, Fig. 2 suggests that the most appropriate theoretical description of the CT-RR exchange experiment hence contains the considered ^{13}C spin pair, ^{13}C that are bonded to the pair of interest and their attached ^{1}H spins. To examine whether this model remains valid for other spin system topologies we present in Fig. 3 results obtained for the Cα–Cδ2 (A) and Cβ–Cε1 (B) spin pairs in L-His · HCl. Again, two-spin simulations (dotted lines) do not adequately reflect the experimental results. The agreement between theory and the experiment is improved by including additional ^{13}C spins. The empirical results are finally well reproduced if ^{1}H spins are taken into account, as indicated in Figs. 3A and B. Note that in both cases the theoretical results not only lead to good overall agreement with the empirical data but even reproduce the high-frequency oscillations detectable in the experiment. In Fig. 3A, nine spins were included in the simulation while eight spins were

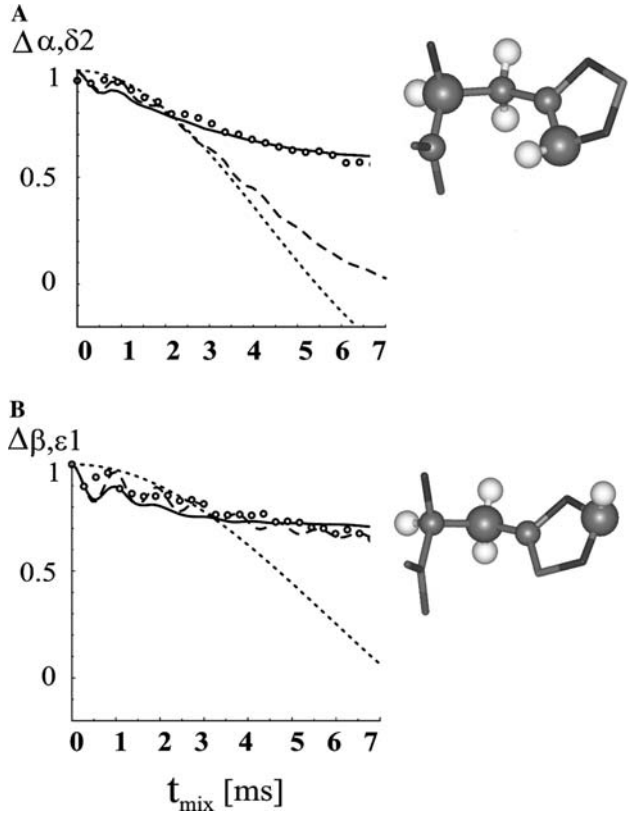

Fig. 3. Comparison between experimental CT-RR transfer curves (symbols) obtained for the Cα–Cδ2 (A) and Cβ–Cε1 (B) spin pair in L-His · HCl. Similar to Fig. 2, dotted lines correspond to QM simulations of a ^{13}C two-spin system, dashed lines reflect the transfer behavior including all ^{13}C spins and the solid line is obtained if the indicated spin system geometry is considered.

sufficient to approximate the experimentally detected behavior in (B).

The results of Figs. 2 and 3 indicate that knowledge of the complete 3D structure allows for an adequate description of the experimentally detected spin dynamics. We note that the agreement between theory and experiment could only be observed using the constant-time version of the RR experiment. A simple qualitative comparison of the three experimentally detected transfer curves in Figs. 2 and 3 suggests that several structural parameters, possibly including the long internuclear distance of interest, affect the spin system dynamics. However, from the results presented so far one cannot conclude whether and to which accuracy CSS transfer methods are helpful in the context of establishing non-trivial structural constraints in uniformly labeled molecules. For this purpose, we conducted an extensive computational study to elucidate which interactions (and hence structural parameters) determine the spin system behavior. The QM simulations shown in Figs. 2 and 3 were repeated for decreasing numbers of internuclear (i.e., through-space distance) constraints within the relevant spin topologies. Dipolar interactions were correspondingly removed from the spin system Hamiltonian until changes in the transfer dynamics were observed. These MS studies led to the following general description of CSS transfer between two homonuclear ^{13}C spins k and l: if the dipolar coupling d_{kl} between two ^{13}C spins k and l is to be investigated, the QM description must include (^{1}H, ^{13}C) and (^{13}C, ^{13}C) interactions to the nearest neighbor carbon and proton spins (Fig. 4). These include one-bond scalar and dipolar interactions from the carbon spins (k, l) to their nearest ^{13}C neighbors $(k, l) \pm 1$. Moreover, heteronuclear scalar and dipolar (^{1}H, ^{13}C) within each subunit (indicated in Fig. 4) and between adjacent units (i.e., maximal over two bonds) must be included. Notably, these local topologies can be defined without a priori knowledge about the 3D structure of the molecule of interest and

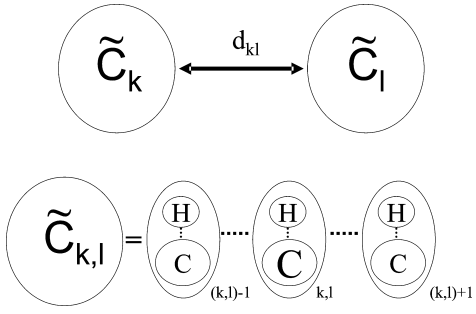

Fig. 4. Generic spin system relevant for the description of CSS transfer between two homonuclear ^{13}C spins k and l and the dipolar coupling d_{kl} of interest. The QM description must include: (1) homonuclear (^{13}C, ^{13}C) one-bond scalar and dipolar interactions from spin (k, l) to its nearest neighbors $(k, l) \pm 1$ and (2) heteronuclear (^{1}H, ^{13}C) scalar and dipolar couplings within each subunit and between adjacent units.

only requires chemical shift assignments for all considered ^{13}C spins. These resonance assignments also would report on additional, unwanted RR conditions that could further complicate the transfer dynamics of interest. Strong interference effects studied in [19] can hence be avoided.

3.2. Accuracy of the determined distance

The previous results indicate that the determination of an internuclear distance d_{kl} between ^{13}C spin k and l can be described by a two-spin interaction between two effective carbon spins that reflects a QM incorporation of the nearest neighbor interactions. These results are in line with a variety of experimental and theoretical studies that predict that the nearest neighbor (i.e., the strongest) interactions determine the spin system dynamics in multiply labeled biomolecules [5,57–62]. We now examine the accuracy with which the internuclear distance of interest can be determined. Unlike to a relaxation analysis, where an independent measurement must unequivocally determine the zero-quantum relaxation rate or the corresponding parameters must be used as a fit parameter, the MS approach directly allows for the variation of the internuclear distance of interest. In Fig. 5, we present numerical results for the three spin geometries considered so far. In all cases, the QM transfer curves clearly remain sensitive to the distance of interest. Moreover, the interatomic distances predicted from the neutron diffraction study [53] most adequately describe in all cases the empirical data. For the relatively short (Cα, Cγ) distance measured in (A), the accuracy suggested by our numerical results is better than ± 0.2 Å. In (B) and (C), where distances of 3.3 and 3.6 Å are expected, respectively, lower bounds of the expected distance can be readily given but the theoretical curves are less sensitive to a decrease of the (^{13}C, ^{13}C) dipolar coupling. For example, varying the distance from 3.3 to 3.7 Å only mildly affects the transfer behavior in (B). A similar behavior is observed for the Cβ–Cε1 constraint (3.6 Å). The numerical simulations hence give a relatively well-defined lower bound for the distance of interest but fail to accurately determine an upper structural bound. For the sake of clarity, only three different spin system geometries were considered in Fig. 5. Additional studies [63] were conducted for the CO–Cβ, the Cβ–Cδ2, and the CO–Cδ2 pairs in L-His · HCl. In all cases, our observations correlate well with the qualitative behavior shown in Fig. 5.

We also performed experiments on a uniformly [^{13}C, ^{15}N]-labeled version of FMOC-arginine and the tripeptide Ala–Gly–Gly (data not shown). In the latter case, we observed deviations in the CO–Cβ transfer curves of alanine which are sensitive to methyl-rotations and hence the absolute size of the Cβ–H dipolar coupling. In line with earlier reports [14] in ^{13}C spin pairs, these

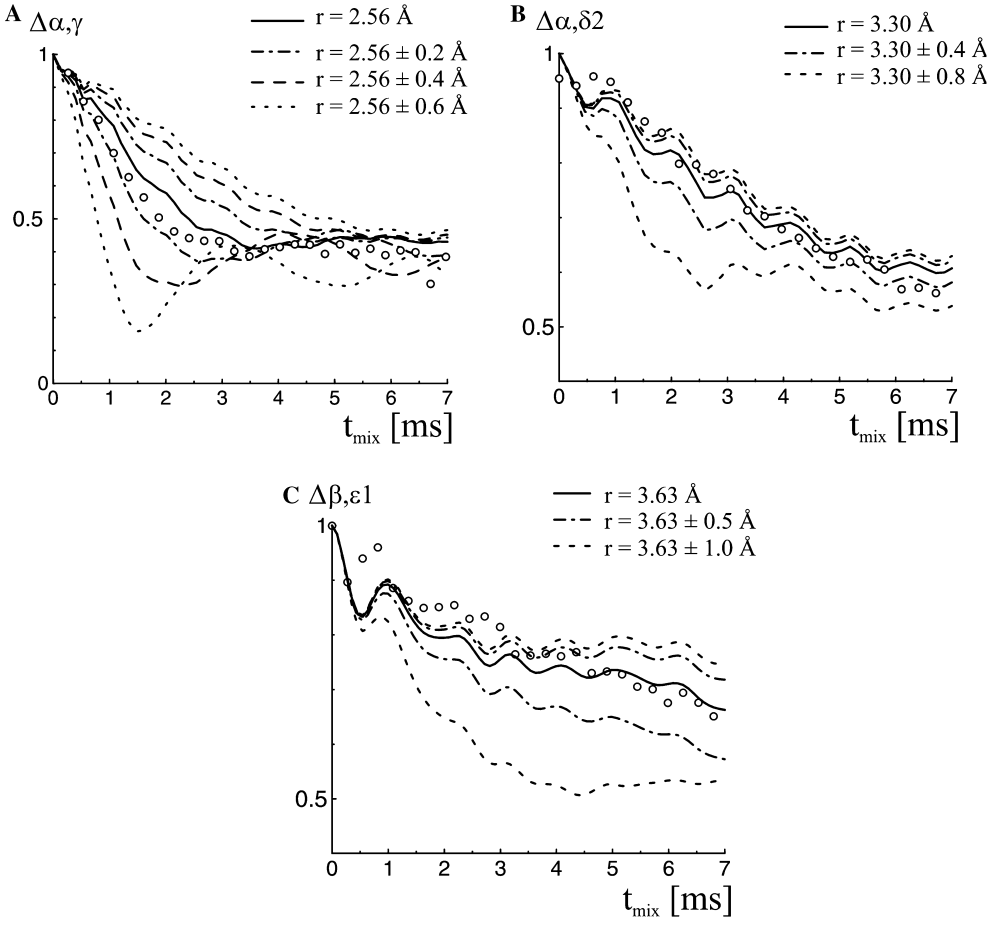

Fig. 5. Comparison between QM transfer curves simulated for different internuclear distances and experimental data points for three different spin pairs in His · HCl. Bold curves correspond to distances as obtained from the neutron diffraction study [53].

observations indicate that (^{1}H, ^{13}C) dipolar interactions strongly affect the details of RR recoupling, in particular if larger (^{13}C, ^{13}C) distances are to be probed. To investigate this aspect in more detail, we present in Fig. 6A RR exchange results for the Cα–Cγ pair in L-His · HCl for three different CW decoupling fields (53, 83, and 125 kHz). In agreement with numerical simulations (indicated as lines in Fig. 6), an increase in decoupling field strength improves the signal modulation due to the dipolar coupling of interest. The same, albeit less pronounced, behavior is observed for the Cβ–Cε1 spin pair in Fig. 6B. Hence the apparent insensitivity of the experimental CT-RR curves for longer distances is strongly affected by next neighbor (^{13}C, ^{1}H) couplings. In general, the accuracy of the distance determination can be improved by increasing the decoupling field strength. In line with earlier observations [14], the RF field strength must be larger under RR conditions than for conventional (off-RR) conditions.

Fig. 6 furthermore indicates that for the reliable detection of internuclear distances of 2.5 Å or larger, strong decoupling fields and long mixing times may be necessary to observe a dipolar oscillation in the dephasing curve. In agreement with the relaxation analysis of [19], our MS approach for example predicts dipolar oscillations for a 2.56 Å distance at a ^{1}H decoupling field of 125 kHz (Fig. 6A). For the 3.6 Å (^{13}C, ^{13}C) distance considered in Fig. 6B, mixing times in the order of several tens of milliseconds and strong ^{1}H decoupling fields would be required. Such conditions were assumed in the theoretical analysis of [19]. In the current context and for a variety of biophysical applications where signal to noise considerations dictate MAS rates, RF decoupling fields and maximum mixing times, the offset in the final difference polarization is determined by relaxation and the presented MS analysis may more appropriately reflect the experimental situation. In particular, the signal decay is predominantly given by insufficient ^{1}H decoupling mediated by (^{1}H,^{13}C) dipolar and through-bond interactions and can be readily analyzed in the proposed MS approach. In addition to the decoupling field strength, false settings in the MAS rate or inhomogeneously broadened single-quantum resonances [16] influence the transfer profile and could be included here. Finally, the determination of internuclear distances using solid-state NMR methods may be

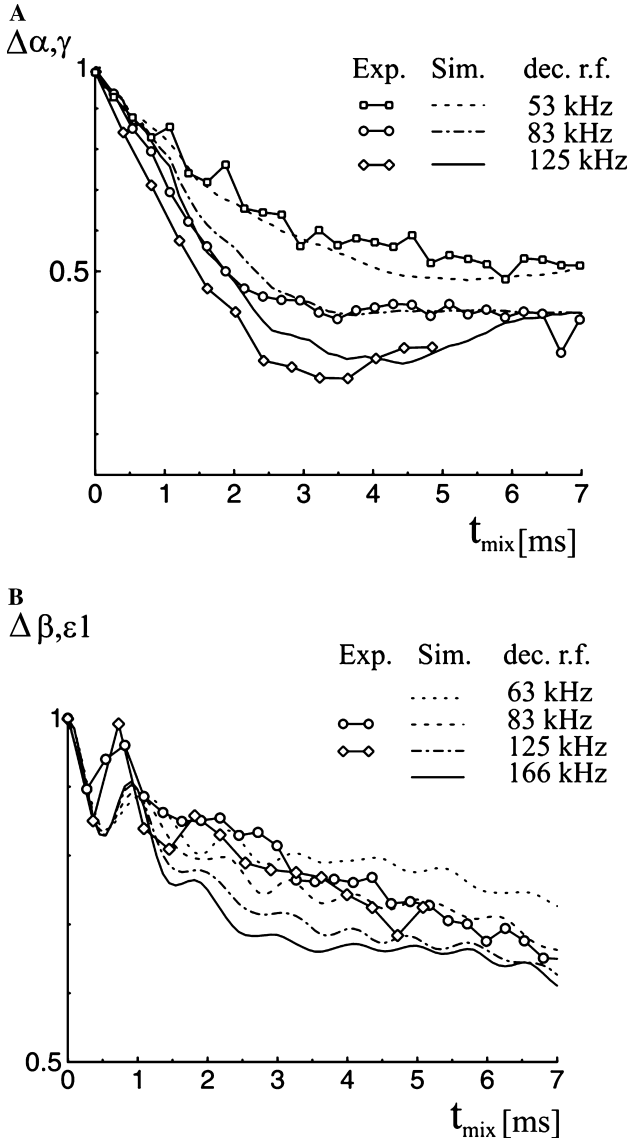

Fig. 6. Comparison between experimental transfer curves (symbols) to numerical simulations (lines) for three different ^{1}H decoupling fields. Exchange curves are shown for the Cα–Cγ pair (A) and the Cβ–Cε1 spin pair (B) in L-His · HCl.

influenced by molecular dynamics. In the framework of an MS analysis, such phenomena may be defined by a set of order parameters for each anisotropic (i.e., dipolar and chemical shielding) interaction. These parameters can be readily determined for known geometries such as one-bond dipolar (^{13}C, ^{13}C) or (^{13}C, ^{1}H) couplings.

3.3. Two-dimensional CT-RRTR experiments

The results obtained so far indicate that CSS transfer can provide distance constraints also in uniformly labeled biomolecules. For this purpose, the effective spin system geometry as indicated in Fig. 4 must be considered in a standard QM multiple-spin simulation. For applications in larger systems, such as the 76-residue protein ubiquitin discussed in the following, the one-dimensional CT-RR experiment becomes impractical. Extending the conventional CT-RR correlation experiment into two spectral dimensions is in principle possible. In this case, the transfer of interest is encoded as a cross-peak intensity that, unless the mixing time is precisely synchronized with the MAS rate, overlaps with auto-correlation peaks resulting from spinning sidebands [64]. A structural interpretation of the observed cross-peak intensity is hence complicated. For this reason, we have utilized the 2D implementation of a CT-RRTR experiment (Fig. 1B) where the generalized recoupling condition of Eq. (3) may be fulfilled for different MAS rates (for any given spin pair) and permits separating both contributions in the 2D spectrum. The experimental concept is exemplified in Fig. 7 for the Cα–Cδ1 spin pair of residue 23 (Ile23) in a uniformly [^{13}C, ^{15}N]-labeled version of ubiquitin. Here, an RF field of 1.25 kHz and MAS rate of 5835 Hz were selected for a mixing time of 5 ms. For all considered spin pairs, resonance assignments were obtained from a series of two-dimensional (^{15}N, ^{13}C) correlation experiments [5] that, in line with previous solid-state NMR studies [24,65–67] on ubiquitin, largely agree with results obtained in the solution-state. As visible from Fig. 7, sideband intensities and the correlation peak of interest are clearly separated.

Similar to the RR case, the MS approach can be readily employed to investigate our experimental results using the effective spin geometries displayed in Fig. 4 and the preparation and detection operators defined in

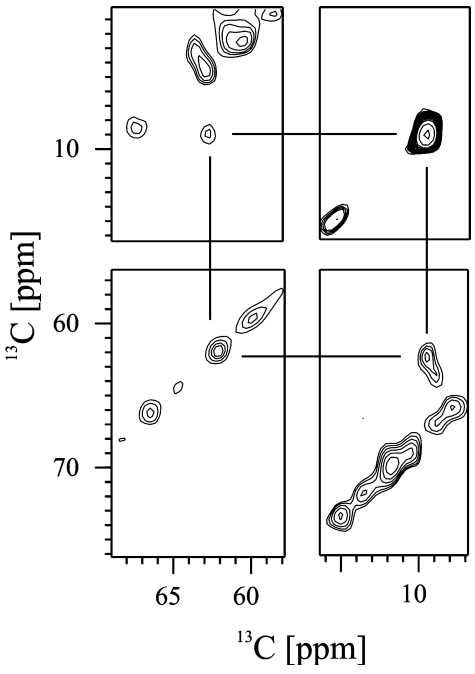

Fig. 7. Sections of a 2D-CT-RRTR experiment for the Cα–Cδ1 spin pair of Ile23 in ubiquitin. Here, an RF field of 1.25 kHz and MAS rate of 5835 Hz were selected for a mixing time of 0.5 ms.

Eq. (6). The spin system topology relevant for Fig. 7 hence involves the examination of an eight-spin system. Since polarization transfer is now experimentally encoded by cross-peak intensities, each mixing time requires the recording of a full 2D spectrum. Experimental results obtained for a mixing times of 0, 5, and 6.5 ms are indicated in Fig. 8 and compared to QM simulations for variable distances (Cα, Cδ1). The numerical results were calibrated using 2D-CT-RRTR reference data obtained for a one-bond Cβ–Cγ distance in ubiquitin. The experimental data hence speak in favor of a 3.5 Å distance in Cα–Cδ1 spin pair, which is in reasonable agreement to the crystal structure (3.0 Å).

Finally, we study the usefulness of the presented approach for the detection of long-range (^{13}C, ^{13}C) distance constraints in ubiquitin. As an example, a 2D RRTR-CT experiment was conducted to examine the (^{13}C, ^{13}C) distance between Ile23–Cδ1 and Leu50–Cβ. For this spin pair, the X-ray structure predicts close contact between both side chains and a corresponding distance of 3.94 Å. As visible from Fig. 9, cross-peaks can indeed be detected for a mixing time of 7 ms. Here, a recoupling field of 1125 Hz and an MAS rate of 5296 Hz was employed. Although the size of the effective spin system (13) in this case does not permit a full QM simulation at present, the observed cross-peak intensity clearly establishes a long-range structural constraint useful for the 3D structure determination of the protein in the solid-state. We have also analyzed other spin pairs (not presented here) that can be grouped in two categories: intra-residue (Thr22 CO–Cβ, Thr55 CO–Cβ, Ile30 Cα–Cγ2, and Ile23 Cα–Cγ1) and interresidue (Ile61 Cγ2–Ser65 Cβ, Ile23 Cγ1–Leu50 Cβ, and Pro19 Cβ–Ser57 Cβ). In all cases, the chemical shifts of the involved spins are well resolved and the contacts expected from the X-ray structure were confirmed through the corresponding cross-peaks in the 2D-CT-RRTR experiments.

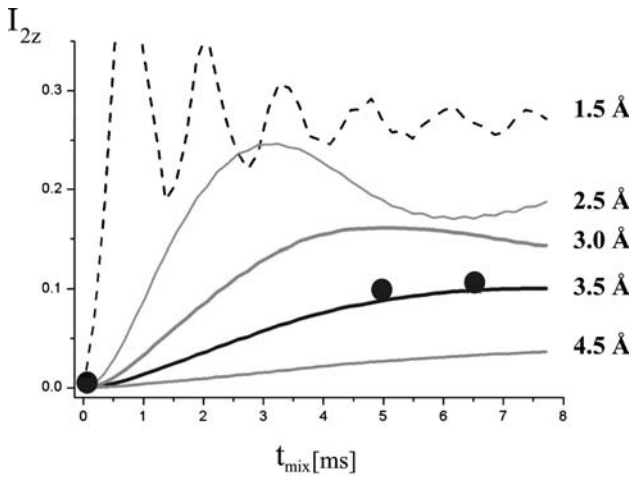

Fig. 8. Comparison between experimental results obtained for a mixing time of 0.5 and 6.5 ms and QM simulations for variable distances (Cα, Cδ1) in ubiquitin. The numerical results were calibrated using 2D-CT-RRTR reference data obtained for the one-bond (Cβ, Cγ) distance of the residues Thr22/Thr55.

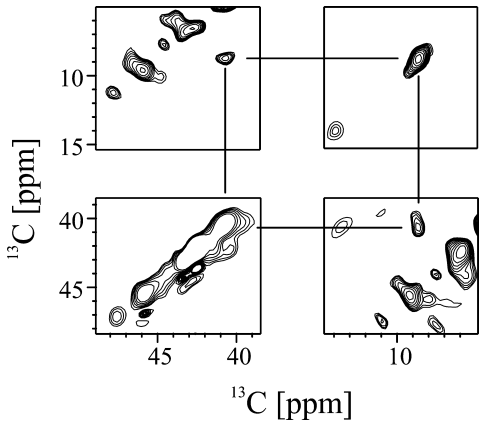

Fig. 9. 2D-CT-RRTR conducted to examine the distance between Ile23–Cδ1 and Leu50–Cβ for a mixing time of 7 ms. A recoupling field of 1125 Hz and an MAS rate of 5296 Hz were employed.

4. Conclusions

Chemical-shift-selective polarization transfer has long been utilized to probe individual structural parameters in solid-state NMR. In contrast to the case of an isotope-labeled spin pair, the application of CSS methods in uniformly labeled molecules requires the consideration of multiple-spin effects. Our study confirms that the corresponding transfer dynamics can be readily computed using a full quantum-mechanical Hilbert-space analysis. These model calculations furthermore reveal that the exchange curves are modulated by nearest neighbor (^{1}H, ^{13}C) and (^{13}C, ^{13}C) interactions but remain sensitive to the internuclear distance of interest. The accuracy of the resulting structural parameters decreases with increasing distance but can be improved by the application of stronger ^{1}H decoupling fields during mixing. Our MS approach is particularly useful to predict the transfer dynamics in the presence of insufficient proton decoupling and inhomogeneously broadened resonance lines. In the limit of infinite ^{1}H decoupling, ^{1}H spins may be removed from the effective spin system topology of Fig. 4 and the MS analysis may be replaced by a relaxation approach.

As demonstrated in the case of ubiquitin, this concept can provide structural constraints useful for the 3D characterization of a uniformly labeled molecule. Although an analysis of the protein conformation solely based on CSS transfer data would be inefficient, a selected set of such (^{13}C, ^{13}C) distance constraints could, for example, complement (^{15}N, ^{13}C) distance parameters determined from REDOR-type [68] correlation experiments [69], dihedral angle constraints obtained from an

analysis of conformation-dependent chemical shifts [70,71] and, finally, interresidue (^{1}H, ^{1}H) distance contacts detected in high-spectral resolution [72,73]. These parameters could subsequently be used in a standard calculation routine that delivers families of molecular conformations consistent with the experimentally derived distance and angle constraints [74]. The number and precision of these parameters determine the accuracy of the resulting 3D structure.

Even if spectral resolution would not permit attribute of cross-peak intensities in a 2D selective correlation experiment to a particular spin pair in the sample, the resulting cross-peak correlations could be utilized as ambiguous structural constraints [75]. CSS-type experiments can also be applied to ^{13}C block-labeled proteins. In this case, the diluted network of ^{13}C spins may, according to our studies, facilitate the analytical interpretation of the selective transfer curves and the extraction of non-trivial (^{13}C, ^{13}C) distances, even in the case of medium-size ^{1}H decoupling fields.

Acknowledgments

Scientific discussions with C.E. Hughes and C. Griesinger are gratefully acknowledged. This work was funded in part by the DFG.

References

[1] M. Mehring, Principles of High Resolution NMR in Solids, second ed., Springer, Berlin, 1983.
[2] E.R. Andrew, A. Bradbury, R.G. Eades, Nuclear magnetic resonance spectra from a crystal rotated at high speed, Nature 182 (1958) 1659.
[3] R.G. Griffin, Dipolar recoupling in MAS spectra of biological solids, Nat. Struct. Biol. 5 (1998) 508–512.
[4] S. Dusold, A. Sebald, Dipolar recoupling under magic-angle spinning conditions, Annu. Rep. NMR Spectrosc. 41 (2000) 185–264.
[5] M. Baldus, Correlation experiments for assignment and structure elucidation of immobilized polypeptides under magic angle spinning, Prog. Nucl. Magn. Reson. Spectrosc. 41 (2002) 1–47.
[6] L.M. McDowell, J. Schaefer, High-resolution NMR of biological solids, Curr. Opin. Struct. Biol. 6 (1996) 624–629.
[7] S.O. Smith, K. Aschheim, M. Groesbeek, Magic angle spinning NMR spectroscopy of membrane proteins, Q. Rev. Biophys. 29 (1996) 395–449.
[8] L.K. Thompson, Solid-state NMR studies of the structure and mechanisms of proteins, Curr. Opin. Struct. Biol. 12 (2002) 661–669.
[9] E.R. Andrew, A. Bradbury, R.G. Eades, V.T. Wynn, Nuclear cross-relaxation induced by specimen rotation, Phys. Lett. 4 (1963) 99–100.
[10] E.R. Andrew, S. Clough, L.F. Farnell, T.D. Gledhill, I. Roberts, Resonant rotational broadening of nuclear magnetic resonance spectra, Phys. Lett. 21 (1966) 505–506.
[11] D.P. Raleigh, M.H. Levitt, R.G. Griffin, Rotational resonance in solid-state NMR, Chem. Phys. Lett. 146 (1988) 71–76.
[12] M.G. Colombo, B.H. Meier, R.R. Ernst, Rotor-driven spin diffusion in natural-abundance C-13 spin systems, Chem. Phys. Lett. 146 (1988) 189–196.
[13] M.H. Levitt, D.P. Raleigh, F. Creuzet, R.G. Griffin, Theory and simulations of homonuclear spin pair systems in rotating solids, J. Chem. Phys. 92 (1990) 6347–6364.
[14] M. Helmle, Y.K. Lee, P.J.E. Verdegem, X. Feng, T. Karlsson, J. Lugtenburg, H.J.M. de Groot, M.H. Levitt, Anomalous rotational resonance spectra in magic-angle spinning NMR, J. Magn. Reson. 140 (1999) 379–403.
[15] O.B. Peersen, M. Groesbeek, S. Aimoto, S.O. Smith, Analysis of rotational resonance magnetization exchange curves from crystalline peptides, J. Am. Chem. Soc. 117 (1995) 7228–7237.
[16] J. Heller, R. Larsen, M. Ernst, A.C. Kolbert, M. Baldwin, S.B. Prusiner, D.E. Wemmer, A. Pines, Application of rotational resonance to inhomogeneously broadened systems, Chem. Phys. Lett. 251 (1996) 223–229.
[17] P.R. Costa, B.Q. Sun, R.G. Griffin, Rotational resonance tickling: accurate internuclear distance measurement in solids, J. Am. Chem. Soc. 119 (1997) 10821–10830.
[18] T. Karlsson, M.H. Levitt, Longitudinal rotational resonance echoes in solid state nuclear magnetic resonance: investigation of zero quantum spin dynamics, J. Chem. Phys. 109 (1998) 5493–5507.
[19] P.T.F. Williamson, A. Verhoeven, M. Ernst, B.H. Meier, Determination of internuclear distances in uniformly labeled molecules by rotational-resonance solid-state NMR, J. Am. Chem. Soc. 125 (2003) 2718–2722.
[20] P.R. Costa, B.Q. Sun, R.G. Griffin, Rotational resonance NMR: separation of dipolar coupling and zero quantum relaxation, J. Magn. Reson. 164 (2003) 92–103.
[21] G. Goobes, G.J. Boender, S. Vega, Spinning-frequency-dependent narrowband RF-driven dipolar recoupling, J. Magn. Reson. 146 (2000) 204–219.
[22] G. Goobes, S. Vega, Improved narrowband dipolar recoupling for homonuclear distance measurements in rotating solids, J. Magn. Reson. 154 (2002) 236–251.
[23] C.M. Rienstra, M. Hohwy, L.J. Mueller, C.P. Jaroniec, B. Reif, R.G. Griffin, Determination of multiple torsion-angle constraints in U-C-13,N-15-labeled peptides: 3D H-1-N-15-C-13-H-1 dipolar chemical shift NMR spectroscopy in rotating solids, J. Am. Chem. Soc. 124 (2002) 11908–11922.
[24] S.K. Straus, T. Bremi, R.R. Ernst, Experiments and strategies for the assignment of fully C-13/N- 15-labelled polypeptides by solid state NMR, J. Biomol. NMR 12 (1998) 39–50.
[25] M. Hong, Resonance assignment of C-13/N-15 labeled solid proteins by two- and three-dimensional magic-angle-spinning NMR, J. Biomol. NMR 15 (1999) 1–14.
[26] A. McDermott, T. Polenova, A. Bockmann, K.W. Zilm, E.K. Paulsen, R.W. Martin, G.T. Montelione, Partial NMR assignments for uniformly (C-13, N-15)-enriched BPTI in the solid state, J. Biomol. NMR 16 (2000) 209–219.
[27] J. Pauli, M. Baldus, B. van Rossum, H. de Groot, H. Oschkinat, Backbone and side-chain C-13 and N-15 signal assignments of the alpha-spectrin SH3 domain by magic angle spinning solid-state NMR at 17.6 tesla, Chembiochem 2 (2001) 272–281.
[28] A. Böckmann, A. Lange, A. Galinier, S. Luca, N. Giraud, H. Heise, M. Juy, R. Montserret, F. Penin, M. Baldus, Solid-state NMR sequential resonance assignments and conformational analysis of the 2×10.4 kDa dimeric form of the *Bacillus subtilis* protein crh, J. Biomol. NMR 27 (2003) 323–339.
[29] T.A. Egorova-Zachernyuk, J. Hollander, N. Fraser, P. Gast, A.J. Hoff, R. Cogdell, H.J.M. de Groot, M. Baldus, Heteronuclear 2D-correlations in a uniformly [C-13, N-15] labeled membrane-protein complex at ultra-high magnetic fields, J. Biomol. NMR 19 (2001) 243–253.

[30] A.F.L. Creemers, S. Kiihne, P.H.M. Bovee-Geurts, W.J. DeGrip, J. Lugtenburg, H.J.M. de Groot, H-1 and C-13 MAS NMR evidence for pronounced ligand–protein interactions involving the ionone ring of the retinylidene chromophore in rhodopsin, Proc. Natl. Acad. Sci. USA 99 (2002) 9101–9106.
[31] A.T. Petkova, M. Baldus, M. Belenky, M. Hong, R.G. Griffin, J. Herzfeld, Backbone and side chain assignment strategies for multiply labeled membrane peptides and proteins in the solid state, J. Magn. Reson. 160 (2003) 1–12.
[32] S. Luca, J.F. White, A.K. Sohal, D.V. Filippov, J.H. van Boom, R. Grisshammer, M. Baldus, The conformation of neurotensin bound to its G protein-coupled receptor, Proc. Natl. Acad. Sci. USA 100 (2003) 10706–10711.
[33] F. Castellani, B. van Rossum, A. Diehl, M. Schubert, K. Rehbein, H. Oschkinat, Structure of a protein determined by solid-state magic-angle- spinning NMR spectroscopy, Nature 420 (2002) 98–102.
[34] K. Nomura, K. Takegoshi, T. Terao, K. Uchida, M. Kainosho, Determination of the complete structure of a uniformly labeled molecule by rotational resonance solid-state NMR in the tilted rotating frame, J. Am. Chem. Soc. 121 (1999) 4064–4065.
[35] K. Nomura, K. Takegoshi, T. Terao, K. Uchida, M. Kainosho, Three-dimensional structure determination of a uniformly labeled molecule by frequency-selective dipolar recoupling under magic-angle spinning, J. Biomol. NMR 17 (2000) 111–123.
[36] C.M. Rienstra, L. Tucker-Kellogg, C.P. Jaroniec, M. Hohwy, B. Reif, M.T. McMahon, B. Tidor, T. Lozano-Perez, R.G. Griffin, De novo determination of peptide structure with solid-state magic-angle spinning NMR spectroscopy, Proc. Natl. Acad. Sci. USA 99 (2002) 10260–10265.
[37] M. Bechmann, X. Helluy, A. Sebald, Selectivity of double-quantum-filtered rotational-resonance experiments in larger-than-two-spin systems, in: S. Kiihne, H.J.M. de Groot (Eds.), Focus on Structural Biology, vol. 1, Kluwer Academic Publishers, Dordrecht, 2001, pp. 23–31.
[38] V. Ladizhansky, E. Vinogradov, B.J. van Rossum, H.J.M. de Groot, S. Vega, Multiple-spin effects in fast magic angle spinning Lee-Goldburg cross-polarization experiments in uniformly labeled compounds, J. Chem. Phys. 118 (2003) 5547–5557.
[39] S.R. Hartmann, E.L. Hahn, Nuclear double resonance in rotating frame, Phys. Rev. 128 (1962) 2042–2053.
[40] A. Pines, M.G. Gibby, J.S. Waugh, Proton-enhanced NMR of dilute spins in solids, J. Chem. Phys. 59 (1973) 569–590.
[41] S.A. Smith, T.O. Levante, B.H. Meier, R.R. Ernst, Computer-simulations in magnetic-resonance—an object-oriented programming approach, J. Magn. Reson. Ser. A 106 (1994) 75–105.
[42] K. Takegoshi, K. Nomura, T. Terao, Rotational resonance in the tilted rotating-frame, Chem. Phys. Lett. 232 (1995) 424–428.
[43] K. Takegoshi, K. Nomura, T. Terao, Selective homonuclear polarization transfer in the tilted rotating frame under magic angle spinning in solids, J. Magn. Reson. 127 (1997) 206–216.
[44] A.E. Bennett, C.M. Rienstra, M. Auger, K.V. Lakshmi, R.G. Griffin, Heteronuclear decoupling in rotating solids, J. Chem. Phys. 103 (1995) 6951–6958.
[45] Y.S. Balazs, L.K. Thompson, Practical methods for solid-state NMR distance measurements on large biomolecules: constant-time rotational resonance, J. Magn. Reson. 139 (1999) 371–376.
[46] G. Metz, X.L. Wu, S.O. Smith, Ramped-amplitude cross-polarization in magic-angle-spinning NMR, J. Magn. Reson. Ser. A 110 (1994) 219–227.
[47] A. Detken, E.H. Hardy, M. Ernst, M. Kainosho, T. Kawakami, S. Aimoto, B.H. Meier, Methods for sequential resonance assignment in solid, uniformly C-13, N-15 labelled peptides: quantification and application to antamanide, J. Biomol. NMR 20 (2001) 203–221.
[48] C.H. Ye, R.Q. Fu, J.Z. Hu, L. Hou, S.W. Ding, C-13 chemical-shift anisotropies of solid amino-acids, Magn. Reson. Chem. 31 (1993) 699–704.
[49] A. Schmidt, S. Vega, The Floquet theory of nuclear-magnetic-resonance spectroscopy of single spins and dipolar coupled spin pairs in rotating solids, J. Chem. Phys. 96 (1992) 2655–2680.
[50] M. Baldus, T.O. Levante, B.H. Meier, Numerical-simulation of magnetic-resonance experiments—concepts and applications to static, rotating and double rotating experiments, Z. Naturfors. A 49 (1994) 80–88.
[51] T.O. Levante, M. Baldus, B.H. Meier, R.R. Ernst, Formalized quantum-mechanical floquet theory and its application to sample-spinning in nuclear-magnetic-resonance, Mol. Phys. 86 (1995) 1195–1212.
[52] Y. Tomita, E.J. Oconnor, A. McDermott, A method for dihedral angle measurement in solids—rotational resonance NMR of a transition-state inhibitor of triose phosphate isomerase, J. Am. Chem. Soc. 116 (1994) 8766–8771.
[53] D. Hohlwein, Photographic neutron-diffraction study of L-histidine Hclh2o by modified Laue method, Acta Crystallogr. Sect. A 33 (1977) 649–654.
[54] S. Vijaykumar, C.E. Bugg, W.J. Cook, Structure of ubiquitin refined at 1.8 Å resolution, J. Mol. Biol. 194 (1987) 531–544.
[55] R.R. Ernst, G. Bodenhausen, A. Wokaun, Principles of Nuclear Magnetic Resonance in One and Two Dimensions, Clarendon Press, Oxford, 1987.
[56] V.B. Cheng, H.H. Suzukawa, M. Wolfsberg, Investigations of a nonrandom numerical-method for multidimensional integration, J. Chem. Phys. 59 (1973) 3992–3999.
[57] M. Baldus, B.H. Meier, Broadband polarization transfer under magic-angle spinning: application to total through-space-correlation NMR spectroscopy, J. Magn. Reson. 128 (1997) 172–193.
[58] S. Kiihne, M.A. Mehta, J.A. Stringer, D.M. Gregory, J.C. Shiels, G.P. Drobny, Distance measurements by dipolar recoupling two-dimensional solid-state NMR, J. Phys. Chem. A 102 (1998) 2274–2282.
[59] S.R. Kiihne, K.B. Geahigan, N.A. Oyler, H. Zebroski, M.A. Mehta, G.P. Drobny, Distance measurements in multiply labeled crystalline cytidines by dipolar recoupling solid state NMR, J. Phys. Chem. A 103 (1999) 3890–3903.
[60] M. Hohwy, C.M. Rienstra, C.P. Jaroniec, R.G. Griffin, Fivefold symmetric homonuclear dipolar recoupling in rotating solids: application to double quantum spectroscopy, J. Chem. Phys. 110 (1999) 7983–7992.
[61] P. Hodgkinson, L. Emsley, The accuracy of distance measurements in solid-state NMR, J. Magn. Reson. 139 (1999) 46–59.
[62] V. Ladizhansky, S. Vega, Polarization transfer dynamics in Lee–Goldburg cross polarization nuclear magnetic resonance experiments on rotating solids, J. Chem. Phys. 112 (2000) 7158–7168.
[63] L. Sonnenberg, Abstandsmessungen an uniform isotopenmarkierten Biomolekülen mit Festkörper-NMR, Georg-August-Universität, Göttingen, 2003.
[64] A.F. Dejong, A.P.M. Kentgens, W.S. Veeman, Two-dimensional exchange NMR in rotating solids—a technique to study very slow molecular reorientations, Chem. Phys. Lett. 109 (1984) 337–342.
[65] M. Hong, K. Jakes, Selective and extensive C-13 labeling of a membrane protein for solid-state NMR investigations, J. Biomol. NMR 14 (1999) 71–74.
[66] A. McDermott, presented at the XXth ICMRBS Conference, Toronto, 2002.
[67] S. Luca, M. Baldus, Enhanced spectral resolution in immobilized peptides and proteins by combining chemical shift sum and difference spectroscopy, J. Magn. Reson. 159 (2002) 243–249.
[68] T. Gullion, J. Schaefer, Rotational-echo double-resonance NMR, J. Magn. Reson. 81 (1989) 196–200.

[69] C.P. Jaroniec, C. Filip, R.G. Griffin, 3D TEDOR NMR experiments for the simultaneous measurement of multiple carbon–nitrogen distances in uniformly C-13, N-15-labeled solids, J. Am. Chem. Soc. 124 (2002) 10728–10742.

[70] H. Saito, Conformation-dependent C-13 chemical-shifts—a new means of conformational characterization as obtained by high-resolution solid-state C-13 NMR, Magn. Reson. Chem. 24 (1986) 835–852.

[71] S. Luca, D.V. Filippov, J.H. van Boom, H. Oschkinat, H.J.M. de Groot, M. Baldus, Secondary chemical shifts in immobilized peptides and proteins: a qualitative basis for structure refinement under magic angle spinning, J. Biomol. NMR 20 (2001) 325–331.

[72] A. Lange, S. Luca, M. Baldus, Structural constraints from proton-mediated rare-spin correlation spectroscopy in rotating solids, J. Am. Chem. Soc. 124 (2002) 9704–9705.

[73] A. Lange, K. Seidel, L. Verdier, S. Luca, M. Baldus, Analysis of proton–proton transfer dynamics in rotating solids and their use for 3D structure determination, J. Am. Chem. Soc. 125 (2003) 12640–12648.

[74] S. Luca, H. Heise, M. Baldus, High-resolution solid-state NMR applied to polypeptides and membrane proteins, Acc. Chem. Res. (2003) in press.

[75] M. Nilges, Ambiguous distance data in the calculation of NMR structures, Fold. Des. 2 (1997) S53–S57.